International Journal of Pharmaceutics 637 (2023) 122892

Contents lists available at ScienceDirect

International Journal of Pharmaceutics

journal homepage: www.elsevier.com/locate/ijpharm

Combining branched copolymers with additives generates stable thermoresponsive emulsions with *in situ* gelation upon exposure to body temperature

A. Rajbanshi [a,d], N. Mahmoudi [b], D. Murnane [a], E. Pavlova [c], M. Slouf [c], C.A. Dreiss [d], M. T. Cook [a,e,*]

[a] School of Life and Medical Sciences, University of Hertfordshire, College Lane Campus, Hertfordshire AL10 9AB, UK
[b] ISIS Muon and Neutron Source, Rutherford Appleton Laboratory, Harwell, Oxford, Didcot OX11 0QX, UK
[c] Institute of Macromolecular Chemistry, Czech Academy of Sciences, Heyrovskeho nam. 2, 16206 Prague, Czech Republic
[d] Institute of Pharmaceutical Science, King's College London, Franklin-Wilkins Building, 150 Stamford Street, London SE1 9NH, UK
[e] UCL School of Pharmacy, University College London, London WC1E 6BT, UK

ARTICLE INFO

Keywords:
Temperature-responsive
Stimuli-responsive
Thermogelling
Neutron scattering
Emulsions

ABSTRACT

Branched copolymer surfactants (BCS) containing thermoresponsive polymer components, hydrophilic components, and hydrophobic termini allow the formation of emulsions which switch from liquid at room temperature to a gel state upon heating. These materials have great potential as *in situ* gel-forming dosage forms for administration to external and internal body sites, where the emulsion system also allows effective solubilisation of a range of drugs with different chemistries. These systems have been reported previously, however there are many challenges to translation into pharmaceutical excipients. To transition towards this application, this manuscript describes the evaluation of a range of pharmaceutically-relevant oils in the BCS system as well as evaluation of surfactants and polymeric/oligomeric additives to enhance stability. Key endpoints for this study are macroscopic stability of the emulsions and rheological response to temperature. The effect of an optimal additive (methylcellulose) on the nanoscale processes occurring in the BCS-stabilised emulsions is probed by small-angle neutron scattering (SANS) to better comprehend the system. Overall, the study reports an optimal BCS/methylcellulose system exhibiting sol–gel transition at a physiologically-relevant temperature without macroscopic evidence of instability as an *in situ* gelling dosage form.

1. Introduction

Thermoresponsive polymer surfactants can produce emulsions which exhibit a reversible sol–gel transition upon heating above a critical temperature (T_{gel}) (Da Silva et al., 2022). These systems have a benefit over traditional pharmaceutical emulsion formulations in that application to the body can occur in a low viscosity state, allowing ease of spreading, spraying, or injecting, amongst other processes (Dumortier et al., 2006). Upon contact with body heat, the emulsion system can transition to a gel state, offering an elastic response to any deformation applied, such as physiological clearance mechanisms (e.g. blinking) or external shear, and an overall improved retention at the target site (Cook et al., 2021; Ward and Georgiou, 2011). As a broad class, thermoreversible gels have been exploited in numerous pharmaceutical and healthcare applications, including topicals (Haddow et al., 2020, 2021; Hussain and Ahsan, 2005), injectables (Swindle-Reilly et al., 2009), and as a platform for cell therapies (Zhao et al., 2016). Whilst thermoreversible gels are typically aqueous polymer solutions (Jeong et al., 2012), the expansion of this class to emulsion systems adds further opportunity in pharmaceuticals. The presence of an oil phase allows better solubilisation of poorly water-soluble molecules which are not typically very soluble in thermoreversible gels. Dispersing the oil phase opens up the potential to further tailor properties of the system such as rates of drug liberation from droplets, rheology of the system, stability, and other factors relating to size such as perceived texture (Aulton, 2013). These thermoresponsive emulsions exhibiting gelation have been formed using several emulsifiers, including proteins (Dickinson and Casanova, 1999), block copolymers (Scherlund et al., 1998), graft

* Corresponding author at: UCL School of Pharmacy, University College London, 29-39 Brunswick Square, London WC1N 1AX, UK.
E-mail address: michael.t.cook@ucl.ac.uk (M.T. Cook).

https://doi.org/10.1016/j.ijpharm.2023.122892
Received 26 January 2023; Received in revised form 12 March 2023; Accepted 23 March 2023
Available online 30 March 2023

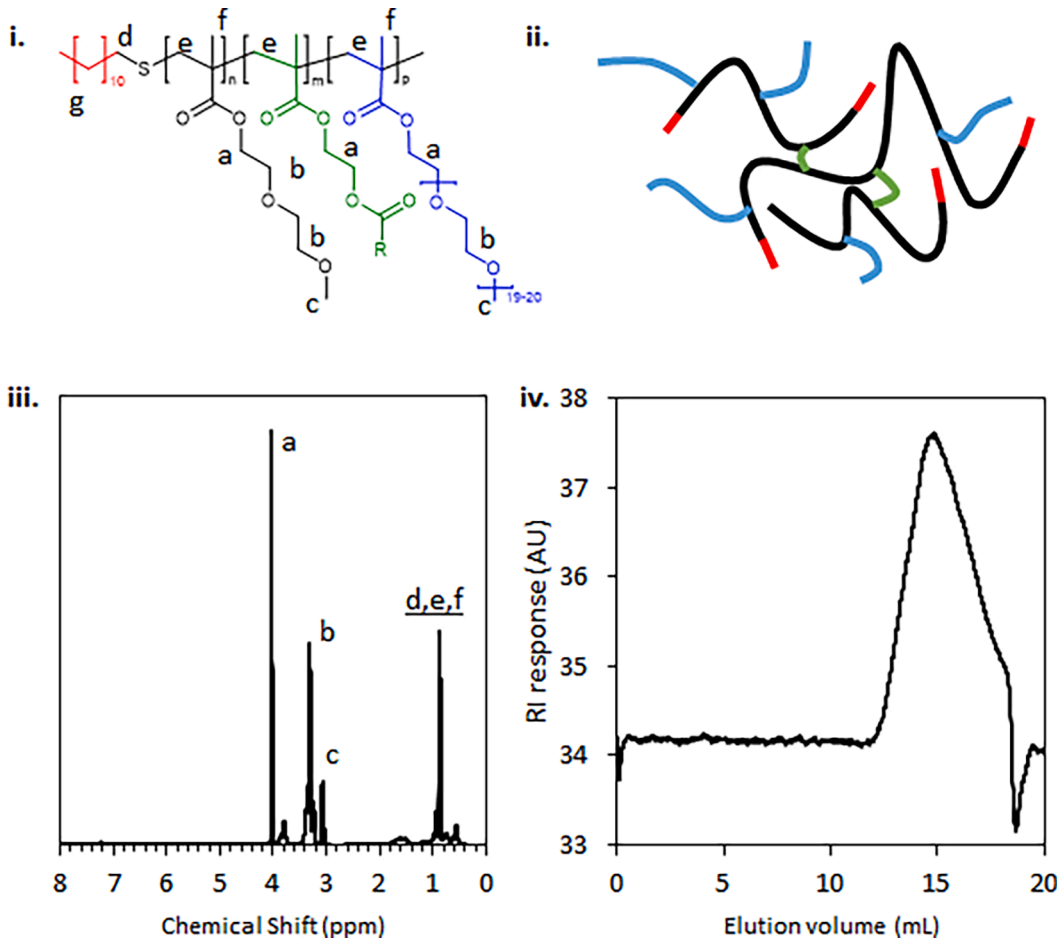

Fig. 1. Chemical structure (R represents another polymer chain to indicate branching) (i) and schematic diagram (ii) of BCS containing DDT (red), DEGMA (black), EGDMA (green), and PEGMA (blue). NMR spectra with overlaid signal allocation (iii) and GPC trace are also shown (iv). (For interpretation of the references to colour in this figure legend, the reader is referred to the web version of this article.)

copolymers (Alava and Saunders, 2004; Koh and Saunders, 2000), and branched copolymer surfactants (BCSs) (Da Silva et al., 2022; Rajbanshi et al., 2022).

BCSs offer a versatile and scalable platform to produce thermoresponsive emulsions. The BCS blueprint exploited previously utilises a "Strathclyde" one-pot synthesis (Baudry and Sherrington, 2006) which has been used successfully for pH-responsive systems (Weaver et al., 2009; Woodward et al., 2009). The elegance of this approach stems from the ability to manipulate BCS properties through the reaction feed mixture, including chain end functionality, molecular weight, co-monomer ratios and degrees of branching, whilst being able to routinely synthesize > 40 g product on a lab scale in a single unoptimized reaction (Rajbanshi et al., 2022). BCSs formed from diethylene glycol methyl ether methacrylate (DEGMA), polyethylene glycol methacrylate (PEGMA), ethylene glycol dimethacrylate (EGDMA) and dodecanethiol (DDT) have recently been reported to produce thermoresponsive "engineered emulsions" which switch from liquid to gel upon heating (Rajbanshi et al., 2022). In these polymers, DEGMA exhibits a "lower critical solution temperature" (LCST) which imparts thermoresponsive behaviour (da Silva et al., 2022; Rajbanshi et al., 2022), PEGMA acts as a steric stabiliser, EGDMA is a cross-linker to induce branching, and DDT is a chain-transfer agent which gives 12-carbon long alkyl chains at the polymer termini (Rajbanshi et al., 2022). This structure is depicted schematically in Fig. 1. DEGMA-based BCS allowed dispersion of dodecane in water which formed an emulsion that creamed over ca 36 h, but was otherwise macroscopically stable (Rajbanshi et al., 2022). The isolated creamed phase exhibited the desired temperature-induced gelation, however for the efficient production of pharmaceutical emulsions, elimination of this creaming event is desirable. Furthermore, the compatibility of these novel emulsifiers with pharmaceutically-relevant oils is unknown.

Emulsion stability, amongst other physical properties, can be enhanced by the use of a secondary co-surfactant alongside the primary surfactant (McClements and Jafari, 2018). Mixing surfactants enables the combination of stabilising factors found in the individual components. For example, combining small non-ionic surfactants with ionic surfactants can lead to a mixed emulsifier film which has the condensed nature typically seen in non-ionic surfactants, with charge repulsion granted by the ionic component (Schulman and Cockbain, 1940). Indeed, many commercial emulsifiers are mixtures of surfactants ("USP Monographs: Emulsifying Wax," 2008). This process of mixing surfactants has the potential to grant this surfactant synergism but also the possibility for antagonism, thus the approach is powerful but complex (McClements and Jafari, 2018). Structural diversity in surfactants includes head group nature (e.g. ionic/non-ionic), tail-group nature (e.g. saturated/unsaturated), and size (e.g. polymeric/small), which overall impact factors such as solubility, ability to pack at an interface, and, in mixed systems, compatibility with any primary surfactant. Additionally, polymeric/oligomeric additives may enhance the stability of emulsion systems by interface stabilisation and by increasing the viscosity of the continuous phase, thus reducing velocities of sedimentation. Thermoresponsive BCS behaviour in mixed surfactant/additive systems is unknown but has the potential to improve emulsion stability, pushing the materials further toward commercial utility.

This study reports the combination of DEGMA BCSs with secondary surfactants and polymeric/oligomeric additives with the aim of generating stable emulsions with the potential for *in situ* pharmaceutical applications. A range of secondary surfactants and additives are explored to determine effects on thermoresponse, compatibility with BCS, and stability. The effect of oil type is also studied to evaluate compatibility of the BCS with pharmaceutically-relevant oils and expand the potential vehicles for drug solubilisation in future. The ability of the BCS-stabilised emulsions to undergo thermoresponsive gelation is assessed by rheology, which allows the determination of the potential for *in situ* gel formation and T_{gel}. Small-angle neutron scattering is employed to probe the nanostructure of the systems, which is fundamental to understanding the bulk properties of the thermoresponsive emulsions.

2. Materials and methods

2.1. Materials

Di(ethylene glycol) methyl ether methacrylate (DEGMA, 95 %), poly (ethylene glycol) methyl ether methacrylate (PEGMA, M_n 950 $gmol^{-1}$), ethylene glycol dimethacrylate (EGDMA, 98 %), 1-dodecanethiol (DDT, 99 %), deuterium oxide (99.9 atom % D), anhydrous dodecane (99 %), tetradecane, mineral oil, sunflower oil, sodium lauryl sulfate, lauryl alcohol, laureth-9, and methyl cellulose (2000 cP, 2 % aqueous solution at 20 °C) were purchased from Sigma-Aldrich (UK). α, α -azoisobutyronitrile (AIBN, >99 %) was obtained from Molekula (UK). Ethanol was supplied by VWR (UK). *n*-Dodecane-d26 (neat) was purchased from QMX (UK). Dialysis tubing with molecular weight cut off (MWCO) of 14 kDa was purchased from Sigma Aldrich (UK). Corn oil was purchased from Acros Organics (UK). Brij 30 and PEG 400 were purchased from Fisher Scientific (UK). Deionised water was employed in all experiments. All chemicals were used as received.

2.2. Synthesis of branched copolymer surfactant (BCS) by free radical polymerisation

The thermoresponsive BCS was prepared with a procedure described previously (Rajbanshi et al., 2022). DEGMA (174 mmol), PEGMA (3 mmol), EGDMA (12 mmol) and DDT (12 mmol) were dissolved in ethanol (190 mL) then bubbled with nitrogen gas for 1 h. Subsequently, a solution of AIBN (1.2 mmol) in ethanol (10 mL) was added. The reaction was then heated to 70 °C and stirred continuously. After 48 h, the reaction mixture was gently distilled at 80 °C to remove ethanol, where rotary evaporation gave foaming. The resultant crude polymer was dissolved in water and transferred to a pre-soaked dialysis bag. The dialysis bag was immersed in deionised water for 7 days and the water was replaced at regular intervals to facilitate the purification process. The resultant polymer solution was subjected to lyophilisation for 48 h to obtain a freeze-dried product (yield 85 %).

^{1}H NMR was used to confirm product formation for the BCS using a Bruker Advance AM 600 NMR instrument with $CDCl_3$ at ambient temperature. Delta 5.3.1 NMR software was used to process the data.

Gel-permeation chromatography was conducted using an Agilent Infinity II MDS instrument equipped with differential refractive index, viscometry, dual angle light scattering and variable wavelength UV detectors. The system was equipped with 2 × PLgel Mixed D columns (300 × 7.5 mm) and a PLgel 5 μm guard column. The eluent was DMF with 5 mmol NH_4BF_4 additive. Samples were run at 1 mL/min at 50 °C. Poly(methyl methacrylate) standards (Agilent EasiVials) were used for conventional and universal calibration between 955,000–550 $gmol^{-1}$. Analyte samples were filtered through a nylon membrane with 0.22 μm pore size before injection. Number-average molar mass (M_n) and dispersity (Đ) values were determined by universal calibration using Agilent GPC/*SEC* software.

2.3. Emulsion formation

Aqueous BCS solutions with concentration of 5, 10, or 20 wt% were prepared in cold water. If required, additives (surfactants/polymer/oligomer) were then added at the concentration stated in the associated results. The mixture was refrigerated with intermittent vortexing every 15 min until a clear solution was obtained. The preparation of oil-in-water emulsions was then carried out by mixing 2.5 g of aqueous BCS solution with 2.5 g of dodecane oil. The mixture was emulsified for 2 min using a Silverson L4R mixer using a 5/8″ micro tubular frame with integral general purpose disintegrating head at 2400 rpm and left to rest for 36 h at room temperature. The creamed phase of the emulsions was then isolated for further analysis. The emulsion mass yield was then defined in equation 1:

$$mass\ \ yield\ \ (\%) = 100 \times \frac{5 - Mass\ \ Water}{5}$$

where "Mass Water" is the mass of the lower phase extracted after creaming for a total sample mass of 5 g. The oil phase volume of creamed region (φ_{oil}) may also be determined by equation 2:

$$\varphi_{oil} = \frac{\left(\frac{2.5}{\rho_{oil}}\right)}{\left(\frac{2.5}{\rho_{oil}}\right) + (2.5 - MassWater)}$$

where ρ_{oil} is the density of the oil and 2.5 is the mass of the oil added in g.

Emulsion droplet size was determined by Laser Diffraction using a Sympatec HELOS/BR QUIXEL. 10 μL of emulsion was added to the dispenser *R*3 cuvette containing 50 mL of water with constant stirring at 1800 rpm. Water was used as reference before sample measurement. All the samples were measured at an optical concentration of approximately 30 %. Trigger conditions were as follows: reference measurement duration – 10 s, signal integration time – 100 ms, trigger timeout – 90 s.

2.4. Rheological evaluation of emulsion systems

The rheological properties of the resulting emulsions were studied using an AR 1500ex rheometer with a Julabo cooling system. Analysis was conducted with a gap size of 500 μm using a 40 mm parallel plate geometry. Samples were placed onto the lower plate and trimmed after lowering of the upper plate to the geometry gap stated. The sample was then enclosed using a solvent trap. Temperature ramps were performed from 20 to 60 °C at 1 °C/min intervals (controlled by a Peltier), with a strain of 0.1 % and a frequency of 6.28 rad/s, following a 2 min equilibration period at 20 °C. The cooling cycle was determined by reducing the temperature from 60 to 20 °C at 1 °C/min intervals, at a strain of 0.1 % and a frequency of 6.28 rad/s. Frequency sweeps were conducted at a shear strain of 0.1 % between 0.628 and 100 rad/s with a 2 min equilibration period at the stated temperature.

2.5. Transmission electron microscopy of BCS solutions

Transmission electron microscopy (TEM) of BCS solutions was conducted with a TEM microscope Tecnai G2 Spirit Twin (FEI, Czech Republic). 10 wt% BCS and 10 wt% BCS with 0.25 wt% methylcellulose were prepared in water as described previously. The specimens for TEM were prepared by dropping 4 μL of sample solution onto a microscopic copper TEM grid (300 mesh) coated with thin, electron-transparent carbon film. After 15 min of sedimentation the excess solution was removed by touching the bottom of the grid with a filter paper (designated the "fast drying method"). This fast removal of solution was performed in order to minimize oversaturation during the drying process (Kolouchova et al., 2022; Stepanek et al., 2012). Subsequently, the particles were negatively stained with uranyl acetate (2 wt% solution dropped onto the dried nanoparticles and removed after 15 s in the same manner as the previous solution). The sample was finally left to dry

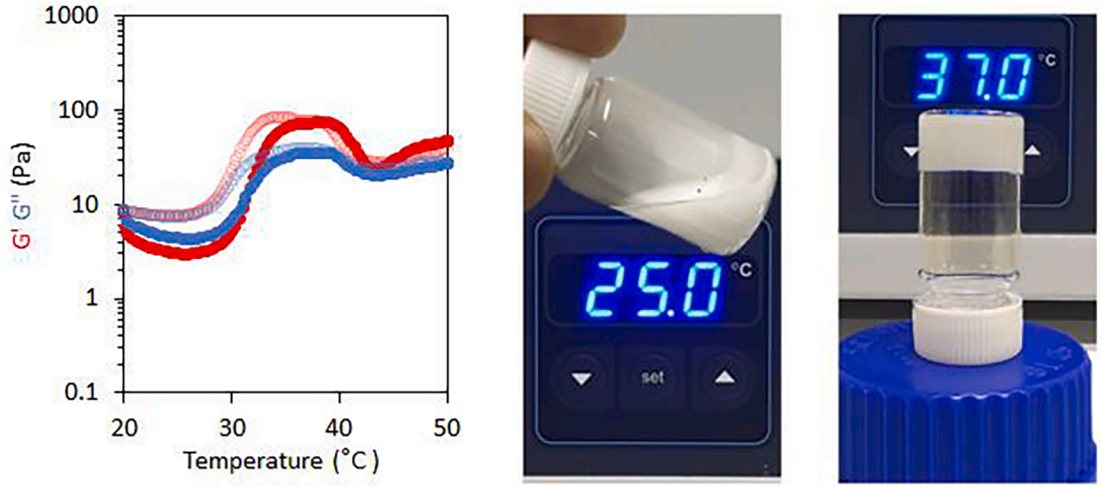

Fig. 2. Small-amplitude oscillatory rheology (left) of emulsions made with dodecane with heating (filled circles) and cooling (open circles) and a fixed angular frequency (6.28 rad/s) and strain (0.1 %) showing G′ (red) and G″ (blue). The emulsions exhibited macroscopic switch (right) from a liquid state (25 °C) to a gel state (37 °C) by vial inversion without any observed syneresis. (For interpretation of the references to colour in this figure legend, the reader is referred to the web version of this article.)

completely and observed with the TEM microscope.

In the next step, the specimens were prepared at elevated temperature using an analogous procedure. The solutions and all tools for sample preparation (grids, tweezers, uranyl acetate solutions etc.) were incubated in an electric oven heated to 40 °C. Then the pre-heated solutions were deposited to the TEM grid and left to sediment for 15 min (the sedimentation took place in the oven at 40 °C). Then the excess solution was removed and the particles were negatively stained with pre-heated solution of uranyl acetate (as described in the previous paragraph) and left to dry completely (again in the oven at 40 °C). With this approach, the sample morphology could be stabilized at elevated temperature and then observed with TEM microscope at laboratory temperature, as documented in previous studies (Kolouchova et al., 2022; Skvarla et al., 2014).

2.6. Small-Angle neutron scattering

SANS experiments were conducted on the time-of-flight diffractometer instrument SANS2d at the STFC ISIS Neutron and Muon Source (UK). Incident wavelengths from 1.75 to 12.5 Å were used at a sample-to-detector distance of 12 m, which gave a scattering vector (q) range from 1.6×10^{-3} to 0.25 $Å^{-1}$. Temperature of the samples was controlled by an external circulating water bath (Julabo, DE). Samples were loaded in 1 cm wide rectangular quartz cells with 1 mm pathlength. Solutions of BCS and BCS with methylcellulose were prepared as described in Section 2.3 in D_2O. Emulsions were then prepared with the addition of deuterated dodecane. The raw SANS data were then processed using wavelength-dependent corrections to the incident spectrum, detector efficiencies, and measured sample transmissions (Heenan et al., 1997). The data were then absolutely scaled to give profiles of scattering intensity I(q) as a function of q, using the scattering from a standard sample (comprising a solid blend of protiated and perdeuterated polystyrene) based on established methods (Wignall and Bates, 1987). All samples were confirmed to be free of multiple scattering. SANS data were fitted using SASView 4.2.2.(www.sasview.org). Where required, scattering length densities (SLDs) were calculated from the monomeric unit using the Neutron activation and scattering calculator website from NIST centre for neutron research ((https://www.ncnr.nist.gov/resources/sldcalc.html)).

2.7. Hot stage light microscopy of emulsions

Light microscopy (LM) of the emulsions at selected temperatures was performed with a LM microscope Nikon Eclipse 80i (Nikon, Japan) equipped with a Linkam THMS600 (Linkam, UK) temperature control stage. A small volume of the emulsion was dropped onto a thin microscopic cover glass, covered with another cover glass and inserted in the temperature control stage. The temperature was increased slowly (1 °C/min) to 25 °C, held for 5 min and LM micrograph was recorded. The same procedure was applied for 30, 35, 40, 45 and 50 °C.

3. Results and discussion

The BCS was successfully synthesised using DEGMA, PEGMA, EGDMA, and DDT (Fig. 1), then used to produce thermoresponsive emulsions. NMR analysis confirmed that the purity of the polymer was > 99.8 % using the residual monomer protons visible at 5.8 and 5.3 ppm against the signal from the polymer backbone (0.5–1.5 ppm), and proton signals were consistent with previous publications (Rajbanshi et al., 2022). GPC confirmed that the BCS had M_n 12.5 kDa with Đ of 4.16, with a monomodal size distribution. From the universal calibration, the average radius of gyration of the BCS was 2.25 nm. A 20 wt% solution of the polymer was then homogenised in the presence of an equal mass of dodecane to disperse the oil phase. This emulsion was then designated to be 10 wt% BCS. The process gave a cloudy dispersion which exhibited creaming. The creamed phase was then isolated after 36 h to give BCS-stabilised emulsions of dodecane-in-water. No further creaming was observed over the duration of the experiments reported. The mass of this creamy phase compared to the initial mass of all components (5 g) was designated to be the yield, in this case 76 %. The final oil phase volume, φ_{oil}, was determined to be 0.72. It should be noted that due to the sample preparation method, these two parameters are inversely proportional to each other.

Rheological analysis of the BCS-stabilised emulsion was conducted. Initially, small-amplitude oscillatory rheology at a fixed frequency was used to study the effect of temperature on the emulsions. This experiment allows the determination of the storage (G′) and loss (G″) moduli at shear strains sufficiently small to lie within the linear viscoelastic region of the system (0.1 % strain), thus retaining the sample structure. The fixed frequency allows for initial investigation of temperature effects alone. The temperature ramp (Fig. 2) shows clear thermoresponsive behaviour in the BCS-stabilised emulsion. At low temperatures, G′ (red)

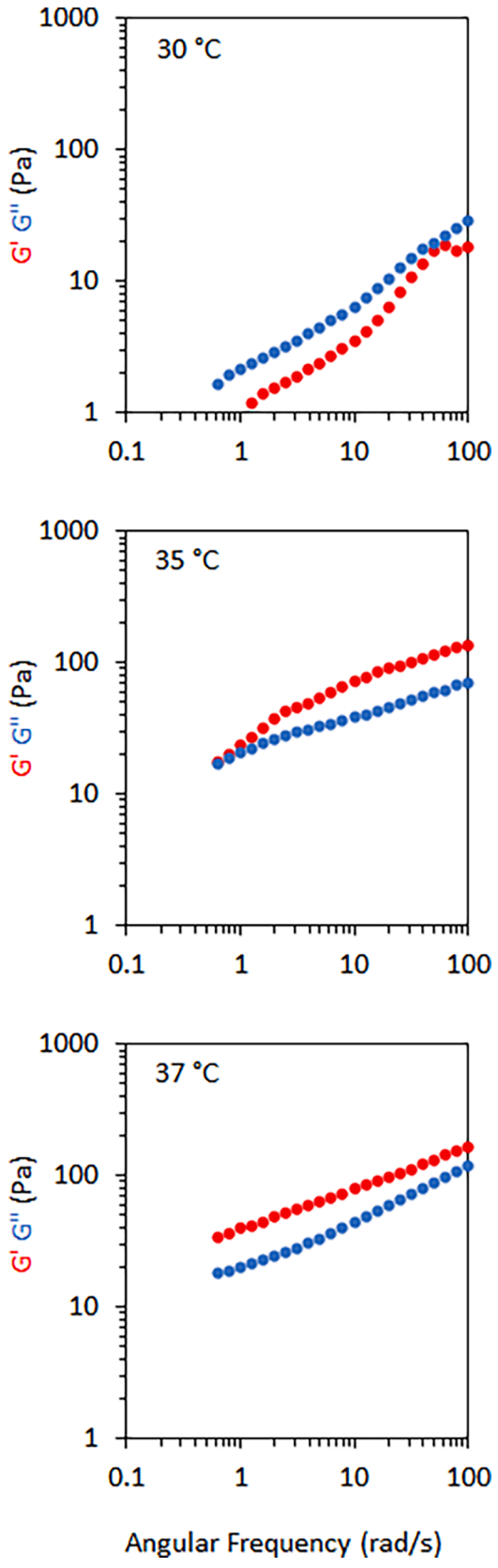

Fig. 3. Rheological behaviour of emulsions stabilised by thermoresponsive BCSs at 10 wt% concentration evaluated by frequency sweeps below (30 °C) and above T_{gel} (35 and 37 °C). G′ is shown in red and G″ is shown in blue. (For interpretation of the references to colour in this figure legend, the reader is referred to the web version of this article.)

Table 1
Yield and oil phase volume (φ_{oil}) of BCS-stabilised emulsions following isolation of the creamed phase.

Oil phase	Density of oil (kg/L)	Yield (wt %)	φ_{oil}	Droplet size (μm)		
				X_{10}	X_{50}	X_{90}
Dodecane	750	76	0.72	1.28	4.00	8.61
Tetradecane	762	78	0.70	1.11	4.17	9.23
Mineral oil	820	80	0.67	1.34	4.13	8.29
Sunflower oil	920	84	0.62	0.85	5.86	17.31
Corn oil	920	84	0.62	0.93	6.12	14.31

and G″ (blue) are low (ca. 3–8 Pa) with the material in a predominantly liquid-like state (G″ > G′). Upon heating above ca. 30 °C, both moduli increase and the system transitions to a predominantly elastic state (G′> G″) at 32 °C, which is a commonly used criterion to indicate gel formation (Constantinou and Georgiou, 2016; Da Silva et al., 2015). As such, 32 °C was designated as T_{gel}. Further heating (above ca. 40°) lowered G′ and G″, which is attributed to reducing interaction between droplets as further kinetic energy is added to the system or structural evolution of the BCS system at higher tempeatures. The sol–gel transition was clearly observed upon heating by vial inversion, without any observable syneresis (Fig. 2). This transition is presumed to arise from the LCST of DEGMA, which is known to be ca 31–35 °C when copolymerised with PEGMA (Bassi et al., 2022). Above T_{gel}, the system reached a plateau at ca 35 °C with a G′ of ca 80 Pa. This temperature makes the emulsion a potential *in situ* gel-former for pharmaceutical applications, where the surface temperature of the body is estimated to be 32–35 °C and internal temperature is 37 °C. The cooling of the system shows a reversibility of this transition with a hysteresis of ca 2 °C. Thus, there is potential for removal of the dosage form by local cooling and extraction.

Small-amplitude frequency sweeps were conducted to evaluate the rheological properties of the BCS-stabilised emulsion above and below T_{gel} (Fig. 3). At 30 °C, below T_{gel}, the emulsion displayed predominantly liquid-like behaviour, with G″ > G′ at all frequencies measured. Upon heating above T_{gel} (35 and 37 °C), two major effects may be noted at both temperatures. Firstly, the emulsions become predominantly elastic at all frequencies, with G′ > G″, which provides further evidence for the formation of a gel state (Zhao et al., 2003). Secondly, the magnitude of both moduli increases ca. tenfold compared to those at T_{gel}, and as such, the overall resistance to deformation of the material increases substantially. At 35 °C, the low frequency region of the rheogram appears to trend toward intersection of the moduli, however no relaxation time was reached within the frequencies measured. At 37 °C the emulsion did not exhibit this reduction in relative elasticity with frequency (i.e. a reduction in loss tangent), and as such, the emulsions stabilised by BCS alone are better suited to internal body sites at 37 °C (such as intravaginal, rectal, and nasal delivery) to reduce any viscous flow over long timescales.

The BCS was then evaluated as an emulsifier for a broader range of oils, to investigate compatibility with oils outside of the model dodecane system (Table 1). Tetradecane was initially explored to probe an oil chain length which was not matched to the C12-terminated BCS. Mineral oil, composed of a mixture of hydrocarbons from crude oil, was also studied to further test the system. Sunflower oil and corn oil were also emulsified with BCS, where these oils are typically composed of triglycerides with greater polarity than simple hydrocarbons (Yara-Varón et al., 2017). Mineral oil, sunflower oil, and corn oil are all used as pharmaceutical excipients and help probe the potential exploitation of BCS in the pharmaceutical industry (FDA Inactive Ingredients Database, n.d.). All oils were successfully emulsified by the BCS at 10 wt% concentration in the emulsion, and the emulsion yield and φ_{oil} were recorded after isolation of the creamed phase (Table 1). Laser diffraction allowed measurement of droplet size distributions, giving X_{10}, X_{50}, and X_{90} values, which correspond to diameter values below which 10, 50

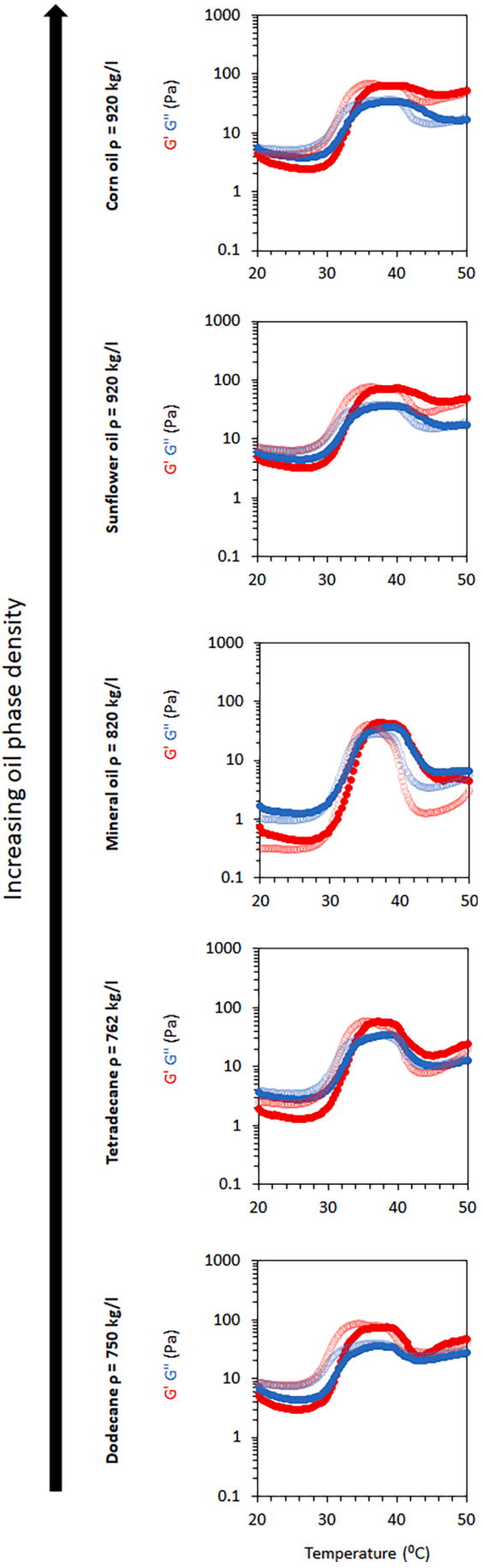

Fig. 4. Small-amplitude oscillatory rheology of emulsions of various oil types with heating (filled circles) and cooling (open circles) and a fixed angular frequency (6.28 rad/s) and strain (0.1 %). G′ (red) and G″ (blue) are shown. (For interpretation of the references to colour in this figure legend, the reader is referred to the web version of this article.)

(caption on next column)

and 90 % of the population are found, respectively. Typically, X_{50}, representing the median is used as an average with the other two values giving a numerical description of dispersity. Full distributions can be found in Fig. S1. Overall, the median droplet size appeared to increase from ca 4 to 6 μm as oil density increased. The mass yield of the creamed phase also increased with the density of the oil, likely due to the velocity of creaming being directly related to the difference in density between the two phases of the emulsion (Hu et al., 2016). Creaming becomes reduced as the density of the oils approach the density of water. This is despite an increase in droplet size, which would typically accelerate the velocity of creaming, highlighting density changes as the dominant factor. Likewise, the final φ_{oil} decreased as the yield increased due to the larger fraction of water in these samples. Overall, the emulsions were effectively stabilised at internal phase volumes >0.5, albeit with the occurrence of creaming.

The oscillatory rheology of BCS-stabilised emulsions was then probed by temperature ramps, as described previously (Fig. 4). The BCS was successful in imparting a sol–gel transition to all emulsified oils studied, without substantial changes to T_{gel}. The plateau region where the gel state ($G' > G''$) was maintained at its maximal value of G′ occurred over a smaller temperature range in tetradecane (33–40 °C) and mineral oil (35–40 °C) relative to dodecane (30–42 °C), however all emulsions were gels at body temperature (37 °C). Sunflower and corn oils appeared to be amenable to sol–gel behaviour, with relatively minor variation in G′ and G″ above T_{gel} (33 °C). These oils are mixtures of triglycerides and minor components such as phospholipids (Yara-Varón et al., 2017). The BCS system is thus both effective at forming emulsions with this range of oils as well as imparting the desired thermoresponsive gelation which can lead to *in situ* gel-forming materials.

Despite successes in generating thermoresponsive emulsions with a diverse range of oils, all the emulsions exhibited significant creaming. Secondary co-surfactants were explored to further stabilise the emulsion systems (Fig. 5). In this study, head group chemistry was explored, using C12 alkyl tail surfactants to match the alkyl chain length on the DDT end groups of the BCS. This increases the likelihood of compatibility of the two tail groups, where mixed small-molecule surfactants are better able to form condensed films at interfaces when tail length is matched (Shiao et al., 1998). The first series of additives explored are lauryl (dodecyl) alcohol, lauryl (dodecyl) sulfate, Brij-30 and laureth-9. Lauryl alcohol has an –OH head group and is selected as a model small non-ionic surfactant with limited steric hinderance in the aqueous phase. Lauryl sulfate is an ionic surfactant used to explore the effect of ionic/non-ionic head group on emulsion behaviour. Brij-30 and laureth-9 are non-ionic surfactants, like lauryl alcohol, but have increasingly long oxyethylene chains as their head group, with degrees of polymerisations of 4 and 9, respectively. This allows the effect of head group size to be explored. A second pair of polymeric/oligomeric additives were also explored, namely, polyethylene glycol (PEG) 400 and methylcellulose, which have a degree of surface activity and can also increase the viscosity of the continuous water phase and reduce the velocity of creaming.

Initially, the first surfactant series (lauryl alcohol, sodium lauryl sulfate, Brij-30 and Laureth-9) were mixed with 10 wt% BCS at increasing surfactant concentration (0.5, 1.0, 1.5 and 2.0 wt%) and homogenised to disperse the oil phase. All mixtures successfully formed emulsions (Table 2), however degrees of creaming, and hence emulsion yields, varied. The final value of φ_{oil} is inversely proportional to the yield, due to the removal of the lower aqueous phase. Overall, the non-ionic surfactants gave a greater yield than the ionic surfactant (sodium

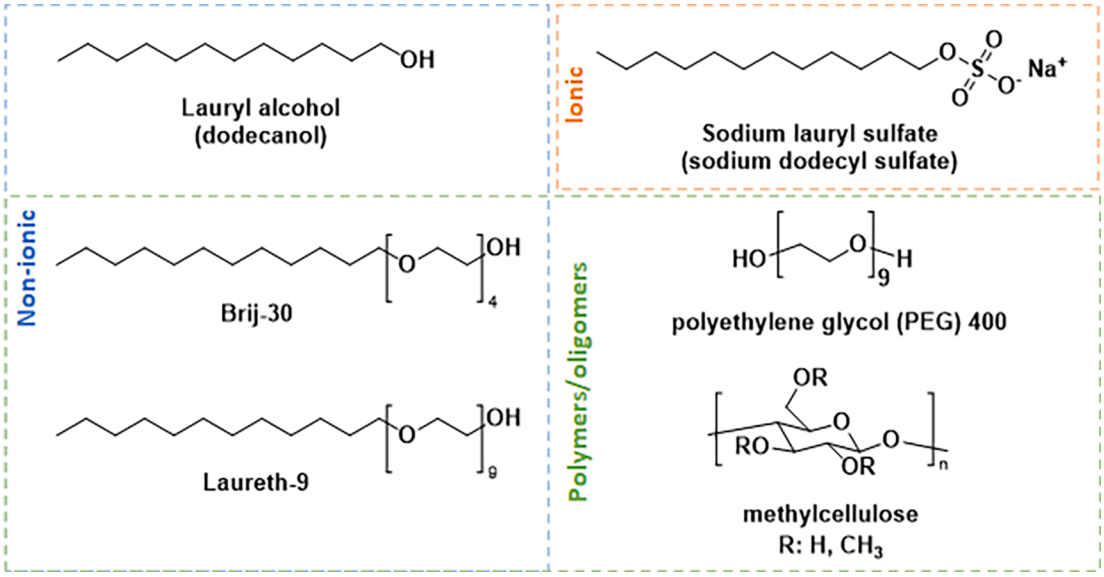

Fig. 5. Chemical structures of additives to BCS-stabilised emulsions.

Table 2
Yield and oil phase volume (φ_{oil}) of BCS/additive emulsions after isolation of the creamed phase at 36 h.

Concentration:	Yield (wt%)				φ_{oil}			
	0.5 wt %	1.0 wt %	1.5 wt %	2 wt %	0.5 wt%	1.0 wt%	1.5 wt%	2 wt %
Lauryl alcohol	86	90	92	94	0.74	0.74	0.72	0.68
Sodium lauryl sulfate	74	74	76	82	0.69	0.66	0.60	0.59
Laureth-9	80	84	94	96	0.65	0.63	0.61	0.60
Brij 30	76	80	90	96	0.72	0.69	0.63	0.59
PEG 400	76	80	84	88	0.72	0.69	0.66	0.64

Table 3
Droplet size of BCS/additive (2 wt%) emulsions after isolation of the creamed phase at 36 h.

Additive (2 wt%)	Droplet Size (μm)		
	X_{10}	X_{50}	X_{90}
Lauryl alcohol	1.38	5.28	9.90
Sodium lauryl sulfate	1.47	4.75	10.74
Laureth-9	1.26	4.23	8.69
Brij 30	1.32	4.40	8.98
PEG 400	1.32	4.08	7.53
Methylcellulose	1.87	3.13	5.35

lauryl sulfate), however all surfactants reduced creaming relative to the BCS alone (yield = 76 %, φ_{oil} = 0.72). Laser diffraction was used to determine droplet sizes of the emulsions (Table 3). Median particle size (X_{50}) of all systems was close to that of BCS emulsions without additive, ca 4 μm. Due to the similarity in droplet size, it is suggested that the homogenisation technique is the major factor that determines the dispesed droplet diameter. Particle size distributions (Fig. S2) indicated a stronger bimodal distribution in the sodium lauryl sulfate system than the other surfactants, with peaks centred on ca 3 and 9 μm. Other systems were largely monomodal with a minor shoulder at lower diameter.

Shear rheology of the BCS/surfactant-stabilised emulsions was then explored with temperature (Fig. 6). Overall, the addition of surfactant appeared to hinder thermogelation events, particularly at concentrations > 0.5 wt%. Lauryl alcohol was the best-performing surfactant, with thermogelation occurring in all samples measured, with T_{gel} ca 33 °C. Comparison with sodium lauryl sulfate showed that the ionic sulfate head group was detrimental to the emulsion relative to the hydroxy group of the lauryl alcohol. Furthermore, increasing the volume of the head group also limited the ability of the emulsion to undergo gelation, completely eliminating the phenomenon at concentrations > 0.5 wt%. All rheograms showed some level of thermoresponsive character, however in the Brij 30, laureth-9, and sodium lauryl sulfate emulsions this was a reduction in viscosity upon heating, which was not of interest in this study. Overall, lauryl alcohol was the most effective cosurfactant, increasing the yield by ca 20 % and allowing the emulsion to undergo thermogelation at a physiologically relevant temperature.

Mechanisms of gelation have been reported in thermoresponsive BCS-stabilised emulsions (Da Silva et al., 2022; Rajbanshi et al., 2022). At low temperatures, BCS is present at both the oil interface and in the bulk as nano-sized oblate ellipsoids. Upon heating, the nano-ellipsoids grow in size due to the LCST of the DEGMA component, driving polymer–polymer associations. In aqueous solutions of BCS, this leads to an increase in viscoelasticity but not gelation (Rajbanshi et al., 2022). At the oil–water interface, a thickening of the stabilising polymer layer occurs due to the LCST effect, drawing polymer from the bulk to the interface (Da Silva et al., 2022). Connectivity between BCS at the interface and BCS in the bulk is critical for gelation to occur. Elimination of thermogelation events in the rheology of the BCS/cosurfactant emulsions (Fig. 6) may be the result of: polymer-surfactant interaction in the bulk affecting the connective polymer aggregates; displacement of BCS from the emulsion surface; or hindering the emulsion droplets from coming into suitable proximity to allow connectivity to occur. As lauryl alcohol did not eliminate thermogelation, it is not believed that polymer-surfactant interaction in the bulk is a dominant effect limiting the ability of the emulsions to undergo gelation. Typically, the interaction of surfactant with thermoresponsive polymer leads to increases in the LCST, which was not observed in this case (Meewes et al., 1991). Thus, the negative effects of sodium lauryl sulfate, Brij-30 and laureth-9 are ascribed to charge and steric effects, respectively, hindering the BCS to connect from one O/W interface, through the bulk, to another. Hypothesised mechanisms for this are displacement of BCS from the interface and hindrance of the droplets from reaching close proximity.

Polymeric/oligomeric additives were then explored for their compatibility with BCS-stabilised emulsions. Both PEG 400 (Table 2) and methylcellulose (Table 4) greatly reduced emulsion creaming. Methylcellulose was particularly effective, eliminating any evidence of

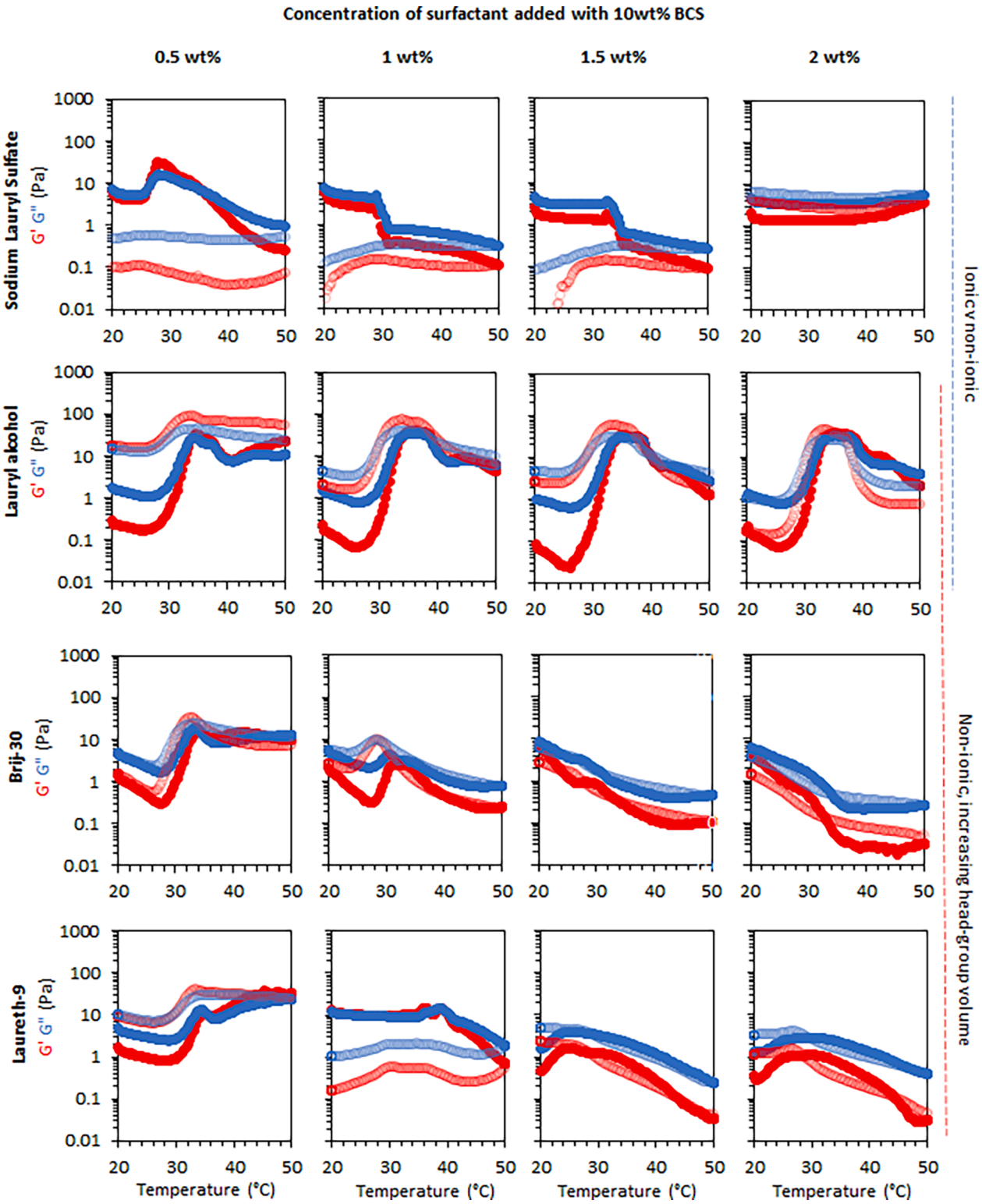

Fig. 6. Temperature-ramp shear rheology of emulsions stabilised with 10 wt% BCS with added surfactant. G′ (red) and G″ (blue) are shown. Closed symbols indicate heating, whilst open symbols indicate cooling. (For interpretation of the references to colour in this figure legend, the reader is referred to the web version of this article.)

creaming by 0.25 wt%, giving a final emulsion with φ_{oil} of 0.57 (Fig. 7). Methylcellulose generated emulsions with the smallest median droplet diameter of any additive (Table 3) with a narrower size distribution (Fig. S2), which is a contributor to the stability of the system. Emulsions stabilised with mixtures of BCS and both additives exhibited the desired themogelation profile (Fig. 8), with T_{gel} of 33 and 30 °C for PEG 400 and methylcellulose, respectively. It is believed that one reason for this effectiveness is that these additives typically form multilayer structures at interfaces rather than monolayers, and thus may be less likely to displace BCS from the interface. There may also be specific synergic effects seen in the BCS/methylcellulose mixtures. Interestingly, methylcellulose extended the G' plateau region over which the gel state was

Table 4
Yield and oil phase volume (φ_{oil}) of BCS/methylcellulose emulsions after isolation of the creamed phase at 36 h.

	Methylcellulose concentration			
	0.1 wt%	**0.2** wt%	**0.25** wt%	**0.5** wt%
Yield	90	98	100	100
φ_{oil}	0.63	0.58	0.57	0.57

Fig. 7. dodecane-in-water emulsions stabilised by BCS alone (10 wt%, left) or BCS/methylcellulose (10/0.25 wt%, right) after 36 h storage at room temperature.

present, up to the highest temperature measured (50 °C) with 0.5 wt% additive concentration. Combining this effect with the stability of the system, methylcellulose was identified as the optimal additive in this study. Once the emulsions were formed they were visually stable for at least 3 months on the benchtop where the use of BCS alone lead to additional creaming over this time period (Fig. S3). In addition, the thermoreversible gel formation in the emulsions stored for 3 months was confirmed by rheology (Fig. S4). The remainder of the study focussed on exploring the properties and structure of this optimised formulation.

The shear rheology of the BCS/methylcellulose (10/0.25 wt%) emulsions was then explored with small-amplitude oscillatory frequency sweeps at temperatures below (25 °C), around (30 °C) and above (35, 37 and 40 °C) gelation (Fig. 9). At 25 °C, the system showed a liquid-like behaviour, with $G'' > G'$. At 30 °C, the emulsion showed a tenfold increase in viscosity and transitioned to a viscoelastic material with a maximum relaxation time of 0.1 s, taken as the inverse of the cross-over frequency between G' and G". At 35–40 °C, the emulsion was predominantly solid-like $G' > G''$ at all frequencies measured. At the highest frequency measured (100 rad/s), G' increased from 42 Pa at 25 °C to 341 Pa at 37 °C, an approximately 8-fold increase in elasticity of the materials. This highlights the potential of the materials as *in situ* gel forming agents in drug delivery.

Transmission electron microscopy (TEM) was initially conducted to probe nanostructures present in solutions of BCS (Fig. 10). At 25 °C the TEM images show exceedingly small objects without clearly defined structure. At 40 °C the appearance of nanoscale objects can clearly be visualised. These nano-objects of ca 10–50 nm dimensions appeared to be a mixture of circular and elongated elliptical objects. As TEM gives a projected two-dimensional shape, it is plausible that these structures are oblate elliptical objects viewed from above, appearing as a circle, and side-on, appearing as an ellipse. A key limitation of the TEM technique is the drying procedure required for imagining to be conducted, thus solution behaviour was probed by SANS.

Small-angle neutron scattering (SANS) was employed to understand the nanostructures present in the emulsions. It is known that thermoresponsive gelation is linked to hierarchical processes occurring at the polymer level, self-assembled nano-aggregate level, and in the supracolloidal assemblies of these aggregates (Blanazs et al., 2009; da Silva et al., 2022). Thus, SANS is a powerful technique to probe nanostructure of aggregates and their interactions underpinning the gel state. In the SANS study, BCS was measured at 20 wt% in D_2O, equivalent to the water phase used in 10 wt% emulsion, at 25, 35, and 45 °C to measure nanostructure below and above the LCST in water alone. Additionally, 0.5 wt% methylcellulose and 20 wt% BCS with 0.5 wt% methylcellulose in D_2O was measured at these temperatures to understand any effect of adding methylcellulose to the structure of BCS. Emulsions of both BCS and BCS/methylcellulose were prepared with deuterated dodecane and D_2O, masking both the water and oil phases in the emulsion system and giving high contrast from polymer in the scattering profile. Scattering profiles required both form factors, which describes the morphology of the scattering objects, and structure factors which account for interactions between the objects.

SANS of solutions of BCS alone show structural transitions with temperature (Fig. 11). At 25 °C the scattering pattern was fitted to an ellipsoidal form factor, consistent with TEM, with uniform scattering length density combined with a power law (Feigin and Svergun, 1987). The polar and equatorial radii of this ellipsoid are 34 by 122 Å, indicating that the ellipsoid is oblate. This is in-line with a previous study of the BCS class (Rajbanshi et al., 2022). In brief, it is hypothesised that steric constraints from the BCS branched structure does not allow the more typical spherical morphology to occur in aggregates of BCS, leading to this oblate morphology. The nano-objects at this temperature, below the LCST transition, are assumed to be formed in water due to the hydrophobic terminal groups driving a self-assembly process into an aggregate. The object has a scattering length density (SLD) of 4.8×10^{-6} Å^{-2}, indicating hydration of the aggregate (SLD PEG: ca 0.88×10^{-6} Å^{-2}, SLD D_2O: 6.37×10^{-6} Å^{-2}).(https://www.ncnr.nist.gov/resources/sldcalc.html). Given the uncertainty around the degree of hydration and the volume fraction of the aggregates formed, fitting was typically attempted using the approximate volume fraction of BCS and conclusions drawn from the value of the SLD are limited. A power law was required to fit the low q region. The exponent of this form factor is −4, indicative of Porod-type scattering arising from objects larger than the q range studied. This can be attributed to larger aggregates or clusters of polymers (Hammouda et al., 2004). When the sample was heated to 35 °C, the upturn at low q disappeared, which is attributed to a larger fraction of the polymer chains forming the well-defined ellipsoidal aggregates. These aggregates have polar and equatorial radii of 88 and 522 Å, respectively, showing growth of the objects, particularly along the equatorial radii. The ellipsoidal form factor required a "sticky-hard-sphere" structure factor, describing hard-sphere interactions with a narrow attractive well (Kotlarchyk and Chen, 1983). At 45 °C the scattering was again fitted with an ellipsoid form factor with a sticky hard-sphere structure factor, albeit with alterations to both the perturbation and stickiness term in the fits. Additionally, at 45 °C the ellipsoids have grown along their equatorial radii (972 Å) with a polar radius nearly unchanged (87 Å). This anisotropic growth has been observed previously for similar BCS systems (Rajbanshi et al., 2022).

Considering the temperature effects on SANS of BCS solutions the following conclusions are drawn:

- At 25 °C, below the LCST, the BCS exist as nano-objects with an oblate ellipsoidal geometry, driven by hydrophobic interactions from

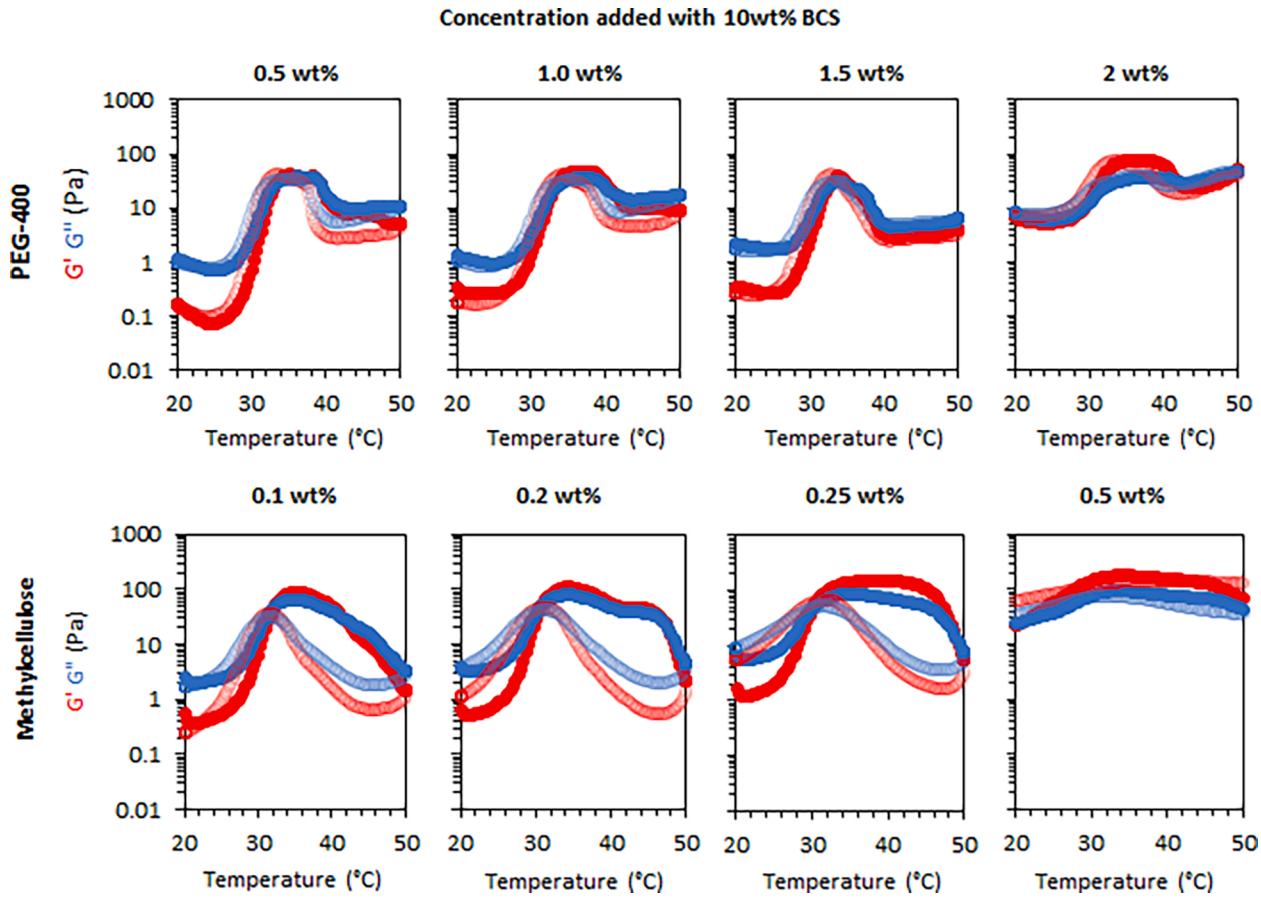

Fig. 8. Temperature-ramp shear rheology of emulsions stabilised with 10 wt% BCS with added PEG 400 or methylcellulose. G′ (red) and G″ (blue) are shown. Closed symbols indicate heating, whilst open symbols indicate cooling. (For interpretation of the references to colour in this figure legend, the reader is referred to the web version of this article.)

DDT (polymer termini). Larger aggregates with sharp interfaces exhibiting Porod scattering are also present.

- At 35 °C, above the LCST, the larger aggregates disappear and the nano-objects present grow larger and more oblate. These aggregates then interact attractively. These effects are attributed to increased hydrophobicity of the constituent BCS above DEGMA LCST.
- At 45 °C, further anisotropic growth of the BCS aggregates occurs with the attractive interactions retained.

SANS of BCS (20 wt%) and methylcellulose (0.25 wt%) were also measured in D_2O to probe the effect of methylcellulose on BCS nanostructure. SANS of methylcellulose (0.25 wt% in D_2O) was also determined to aid comprehension of the system, however no signal was observed in the *q* range studied (Fig. S5). Thus, it is assumed that any changes to the neutron scattering patterns observed, relative to the BCS system, are due to interactions between the BCS and methylcellulose, rather than to the scattering of methylcellulose aggregates. Initial observation of the SANS for the BCS/methylcellulose solutions shows only minor changes from BCS alone (Fig. 11ii). At all temperatures, the BCS and BCS/methylcellulose SANS data are nearly superimposable, except for a small broadening of the correlation peak at 0.01 Å for the 35 °C sample and changes to the low q region at 45 °C. Only minor alterations to the fitting parameters were required (Figs. S6-S8). Thus, there is no evidence of major structural alterations to BCS in aqueous solution upon addition of methylcellulose in the temperature range studied.

SANS of BCS-stabilised emulsions was also conducted at 25, 35, and 45 °C (Fig. 12). In this experiment, both the oil and water phases were deuterated, and scattering is dominated by BCS at the interface and in the bulk where the difference in SLD between the deuterated dodecane and D_2O phases is small (6.71 vs 6.37 $\times$ 10^{-6} $Å^{-2}$, respectively). All emulsions exhibited features consistent with the BCS solutions alone but with lower scattering intensity. This is indicative of a reduced concentration of BCS in the bulk which is attributed to a fraction of the BCS moving to the O/W interface and losing structure, as well as a reduction in the volume fraction of water due to the emulsion system. Other thermoresponsive polymers, such as poly(*N*-isopropyl acrylamide), are known to move to interfaces and lose structuration as they spread across the interface (Li et al., 2013; Zhang and Pelton, 1996). Furthermore, study of structurally related poly(*N*-isopropylacrylamide) BCS by neutron reflectivity at the perfluorooctane/water interface demonstrated the ability of the BCS architecture to move to this interface (Da Silva et al., 2022). At 25 °C, the emulsion's scattering could be fitted using the same parameters (SLD, equatorial/polar radii) as the BCS in solution, but with a reduced volume fraction of 0.056. It is known that the volume fraction of water in the system is 0.34; if the volume fraction of BCS in this water phase was unchanged by the emulsification process it would give an overall BCS volume fraction in the emulsion of 0.068. Thus, there is a ca. 18 % reduction in BCS volume in the bulk water after emulsion formation. At 35 °C, the data could again be fitted with the parameters from the BCS solution with a reduced scale, associated with a reduced volume fraction, relating to the ellipsoid form factor. However, the appearance of an upturn at low *q* was observed, which fits to a power law with a -4 exponent. This is assumed to arise from the emulsion droplets themselves. At 45 °C, a similar effect was observed. Fitting was adequately conducted using the parameters from the BCS solution at 45 °C but with a reduced scale (0.052). An upturn at low *q* was again fitted to a -4 exponent power law. Parameters from all fits are shown in

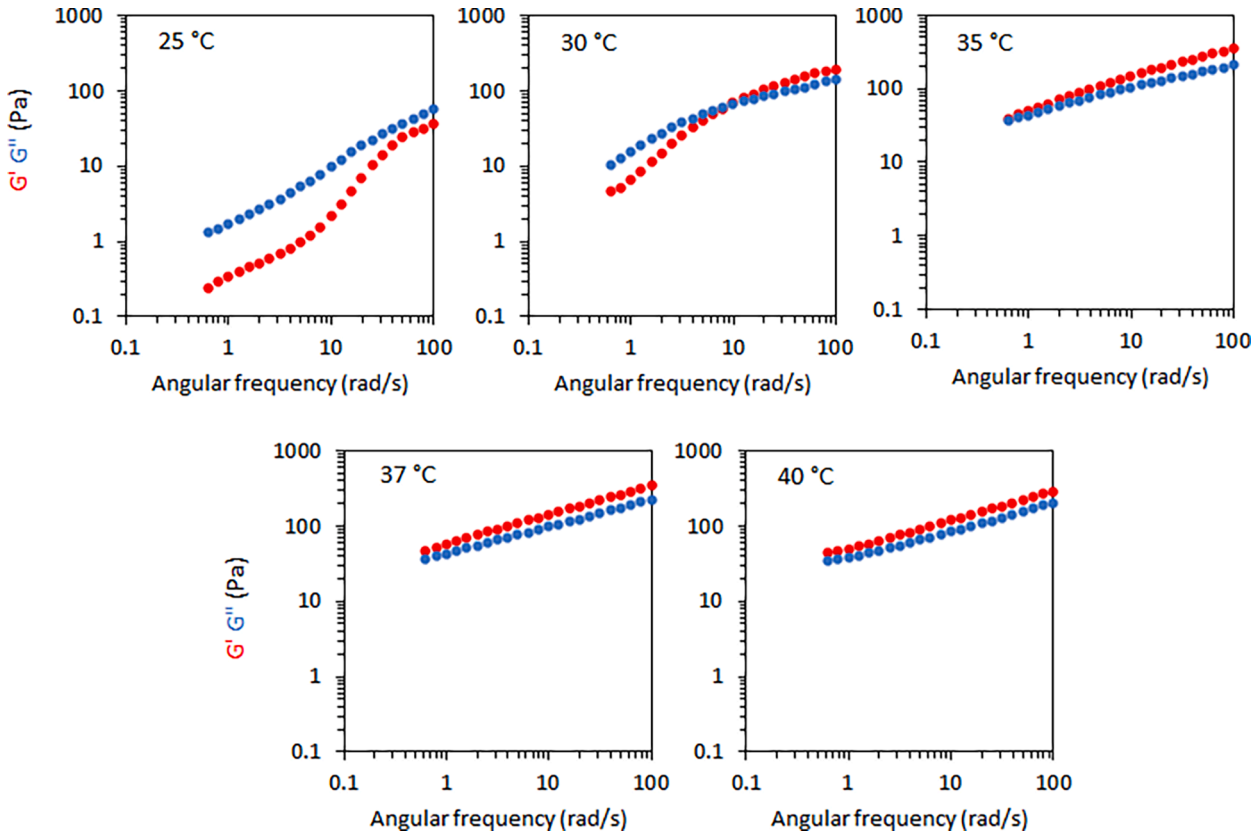

Fig. 9. Rheological behaviour of emulsions stabilised by thermoresponsive BCSs at 10 wt% concentration with 0.25 wt% methylcellulose evaluated by frequency sweeps below (25 and 30 °C) and above T_{gel} (35, 37, and 40 °C). G′ is shown in red and G″ is shown in blue. (For interpretation of the references to colour in this figure legend, the reader is referred to the web version of this article.)

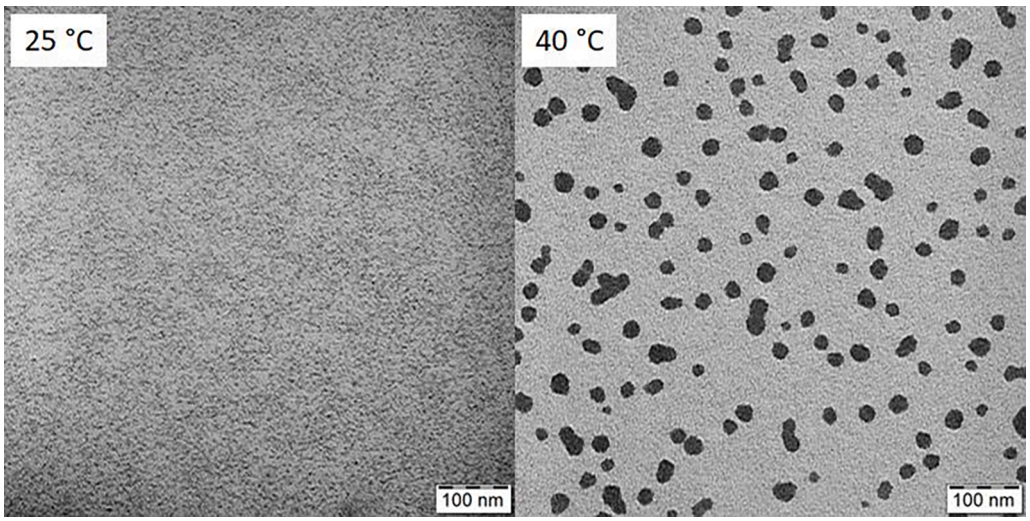

Fig. 10. TEM micrographs of BCS dried at 25 °C and 40 °C, indicating transition from small clusters to larger nano-objects.

supplementary information (Fig. S6-S8, Table S1).

Finally, the BCS plus methylcellulose emulsions were studied by SANS with increasing temperature. At 25 °C, a similar trend was seen as for the BCS emulsion alone. The emulsion's scattering could successfully be fitted with the same parameters as the solution with a reduced scale. At 35 °C, the mixed system could again be fitted with this approach, however the correlation peak moved from $q = 0.00727$ in the BCS emulsion alone to $q = 0.01068$ upon addition of methylcellulose to the emulsion system. This corresponds to distances (d) of 864 and 588 Å before and after methylcellulose addition, respectively, using the relationship $d = 2\pi/q$. At 45 °C the SANS could again be fitted to an ellipsoidal form factor with a sticky hard-sphere structure factor combined to a power law (-4) appearing at low q. The dimensions of this aggregate were fitted using the parameters for the solution alone. Relative to the BCS emulsion alone; this fitting required a reduction in effective radius from 800 to 176 Å.

Considering the SANS data from the emulsions as a whole, the following conclusions are drawn:

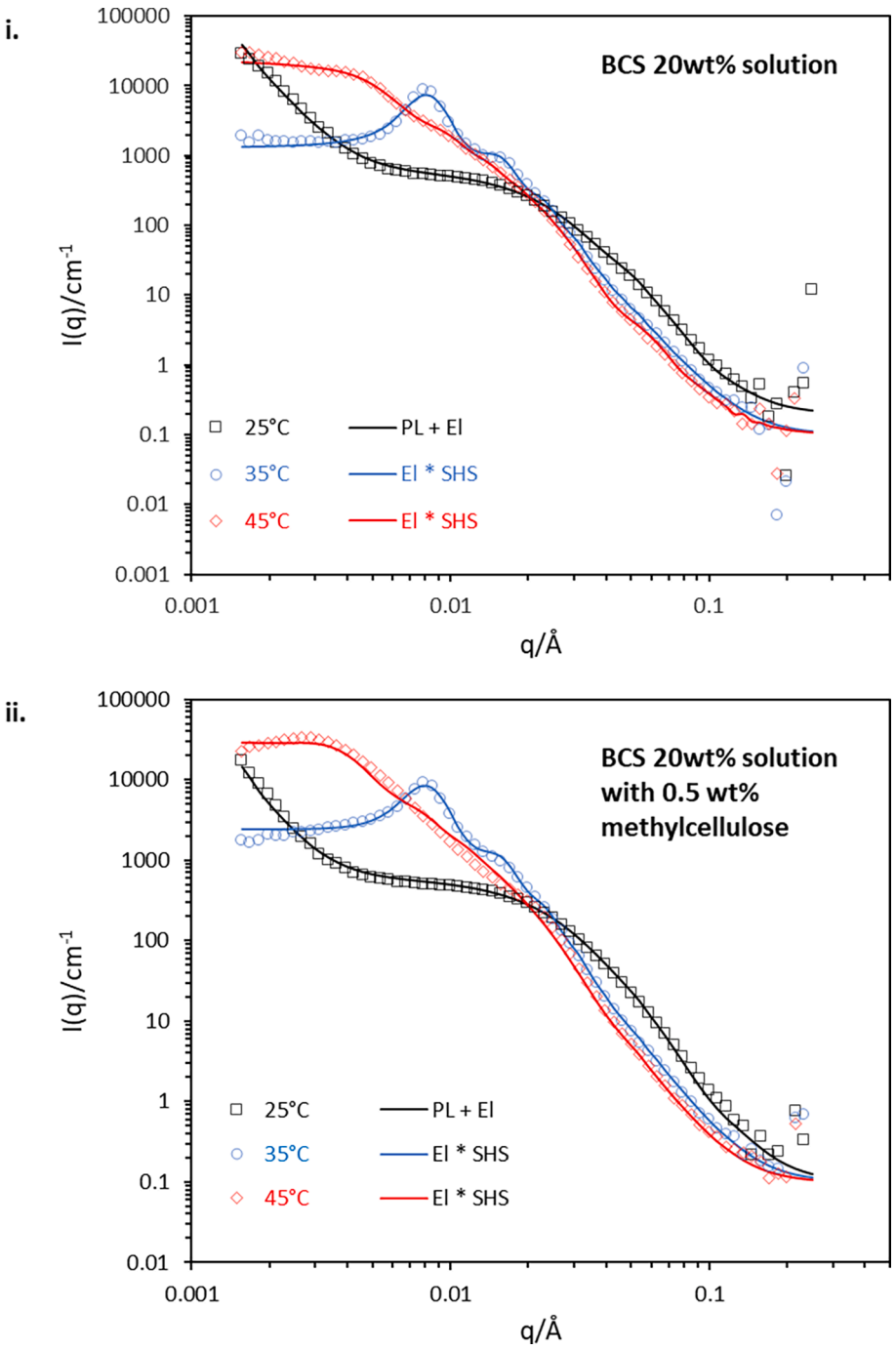

Fig. 11. SANS of BCS solutions (20 wt%) in D_2O (i) and in D_2O with methycellulose added (0.25 wt%) (ii). Data presented at 25, 35, and 45 °C in black, blue and red symbols, respectively. Fits to data are shown as continuous lines, with the models used shown in the legend. EL is an ellipsoid, PL is a power-law, SHS is the sticky-hard-sphere structure factor. (For interpretation of the references to colour in this figure legend, the reader is referred to the web version of this article.)

- Nanoscale aggregates formed in aqueous solutions of BCS and BCS with methylcellulose are preserved in the emulsion system. However, there is evidence that larger structures are also present due to the upturn at low q, which may arise from aggregates or more likely the interface of the oil droplets, outside the q-range measured.
- A reduction in effective concentration of the nanoscale aggregates occurs, which provides evidence for movement of BCS to the oil/water interface and reduction of the structured scattering objects in the bulk.
- The addition of methylcellulose to the emulsions appears to reduce the effective distance between BCS aggregates whilst preserving their nanostructure.

Finally, dodecane-in-water emulsions stabilised by 10 wt% BCS alone and with 0.25 wt% methylcellulose were imaged by light microscopy (LM) with a hot stage to observe possible morphological changes on the microscale as a function of temperature (Fig. 13). The droplet size of BCS-stabilised emulsions was polydisperse with a range ca 6–38 μm, whilst the droplet size of the BCS/methylcellulose emulsions was significantly reduced with the majority at 4–5 μm. This reduction in droplet size explains prior observations that creaming was greatly reduced in the BCS plus methylcellulose emulsion. The emulsions were heated from 25 to 35, then 40 °C to evaluate the system below and above the gelation temperature. No distinct changes were observed in droplet size or morphology, and no additional objects were observed in the

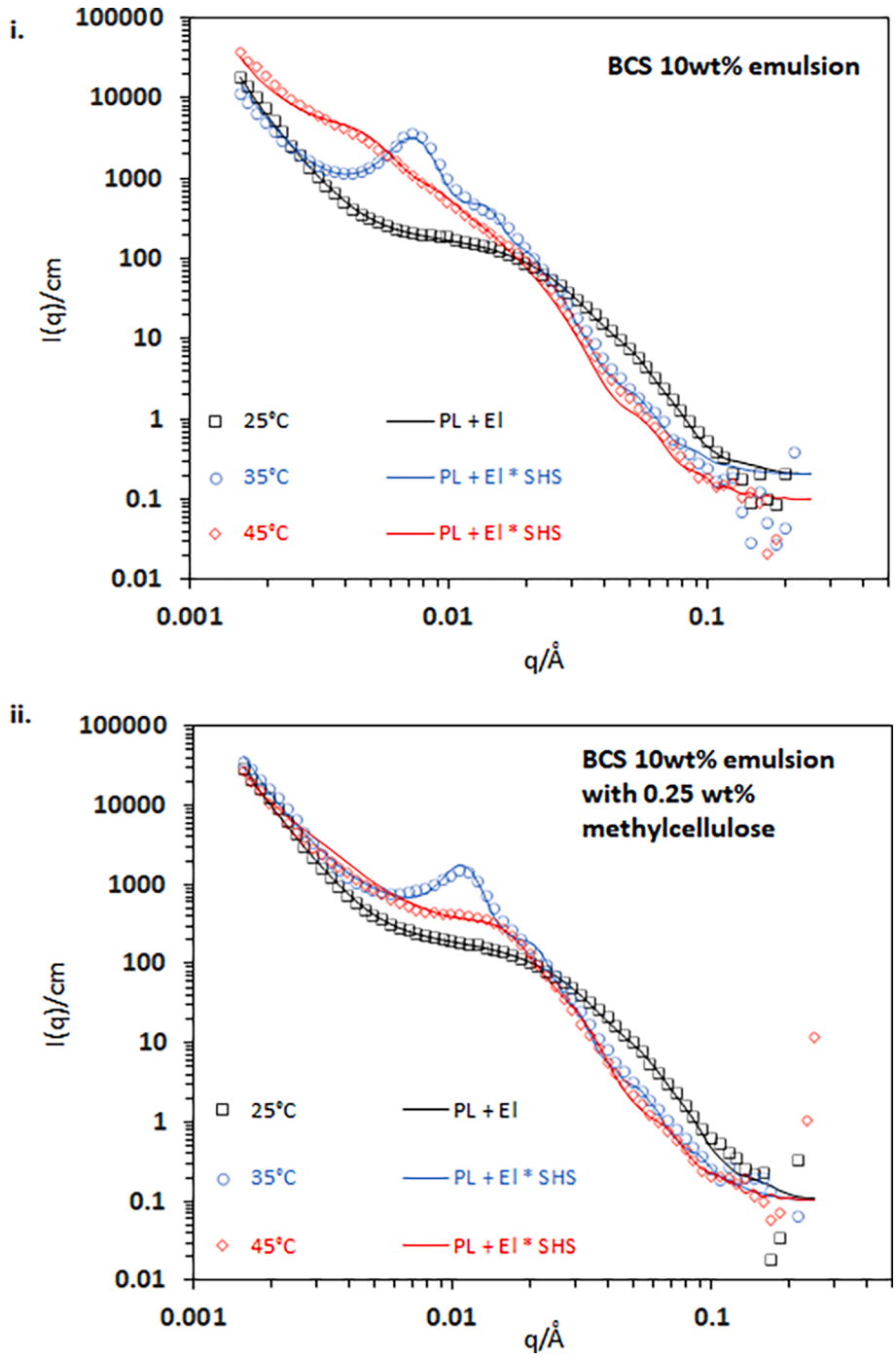

Fig. 12. SANS of BCS emulsions (10 wt%) in D_2O (i) and in D_2O with methylcellulose added (0.25 wt%) (ii). Data presented at 25, 35, and 45 °C are in black, blue and red symbols, respectively. Fits to the data are shown as continuous lines, with the models used shown in the legend. EL is an ellipsoid, PL is a power-law, SHS is the sticky-hard-sphere structure factor. (For interpretation of the references to colour in this figure legend, the reader is referred to the web version of this article.)

heated system. The rheological features observed are therefore not strongly attributed to any changes to the droplets themselves.

4. Conclusions

BCS synthesised by free radical polymerisation of DEGMA, PEGMA, EGDMA, and DDT is effective as an emulsifier for oil-in-water emulsions whilst imparting temperature-responsive gelation to the emulsion systems. This transition occurs at ca 32 °C, making these thermoresponsive emulsions attractive for *in situ* gelation upon contact with body sites and thus exploitation in pharmaceuticals where the gel state may enhance retention at the target site. The BCS was able to both stabilise and impart thermoresponsive behaviour to a range of pharmaceutically-relevant oils. The addition of small molecule surfactants and polymer/oligomer additives to BCS emulsions was explored to reduce instability due to creaming. An optimal formulation of BCS with methylcellulose was identified which eliminated creaming over the experimental period and extended the range of temperatures over which the gel state was stable. SANS study of the system allowed the investigation of the nanostructure, which underpins the rheological response to temperature. BCS in solution formed nanoscale oblate ellipsoidal aggregates which grew and interacted with each other when heated. In aqueous solution, there was

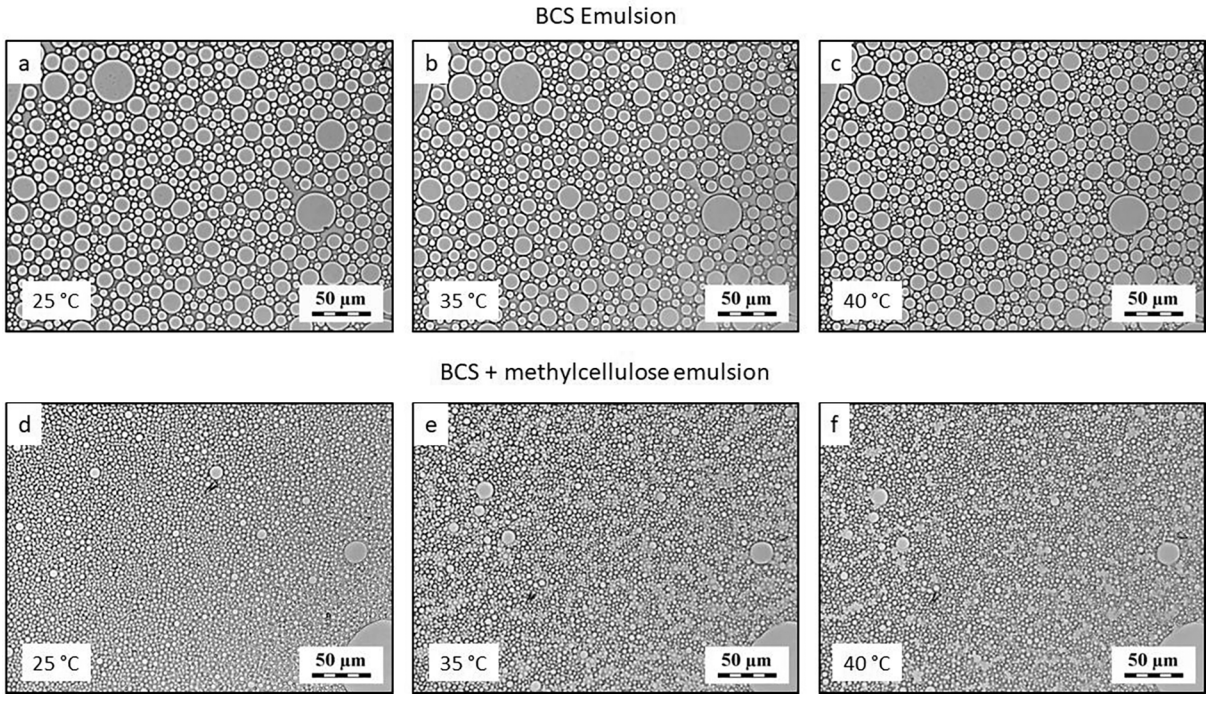

Fig. 13. Light microscopy (LM) images of dodecane-in-water emulsions stabilised by 10 wt% BCS alone (a–c) and with 0.25 wt% methylcellulose (d–f) at different temperatures at 20x magnification.

limited evidence of methylcellulose affecting the nanoscale organisation, however, in the emulsion systems, a different effect was observed. Both the BCS and the BCS/methylcellulose mixed emulsions retained the nanostructures observed in solution but with larger aggregates present. Methylcellulose appeared to reduce the distance between BCS aggregates, tentatively assigned to additional steric crowding in the aqueous phase. Overall, this study reports a novel thermoresponsive emulsion formulation for use as an in-situ gel forming dosage form, along with comprehension of nanostructural mechanisms in the system. Future studies will seek to incorporate the material into delivery devices and explore the effect of processing on performance of the emulsion.

CRediT authorship contribution statement

A. Rajbanshi: Investigation, Methodology, Formal analysis, Writing – original draft, Conceptualization. **N. Mahmoudi:** Investigation, Methodology, Writing – review & editing. **D. Murnane:** Methodology, Writing – review & editing, Supervision, Conceptualization. **E. Pavlova:** Investigation, Methodology. **M. Slouf:** Formal analysis, Writing – review & editing, Methodology. **C.A. Dreiss:** Methodology, Writing – review & editing, Supervision, Conceptualization. **M.T. Cook:** Methodology, Formal analysis, Writing – review & editing, Supervision, Conceptualization.

Declaration of Competing Interest

The authors declare that they have no known competing financial interests or personal relationships that could have appeared to influence the work reported in this paper.

Data availability

Data will be made available on request.

Acknowledgements

The EPSRC are thanked for funding this research (EP/T00813X/1). The grant is also supported by equipment funded by the Royal Society Research Grant (RF17-9915). We gratefully acknowledge the Science and Technology Facilities Council (STFC) for access to neutron beamtime at ISIS, and also for the provision of sample preparation facilities (experiment 2220037, Doi10.5286/ISIS.E.RB2220037).

Appendix A. Supplementary material

Supplementary data to this article can be found online at https://doi.org/10.1016/j.ijpharm.2023.122892.

References

Alava, C., Saunders, B.R., 2004. Effect of added surfactant on temperature-induced gelation of emulsions. Langmuir 20, 3107–3113.
Aulton, Michael E., 2013. Aulton's Pharmaceutics, Harcourt Publishers Limited, London. Doi10.1007/s13398-014-0173-7.2.
Bassi, J., Haddow, P., Luciano, M., Thomas, M., 2022. Thermoresponsive poly (di (ethylene glycol) methyl ether methacrylate) - ran- (polyethylene glycol methacrylate) graft copolymers exhibiting temperature-dependent rheology and self-assembly. J. Mol. Liq. 346, 117906.
Baudry, R., Sherrington, D.C., 2006. Synthesis of highly branched poly(methyl methacrylate)s using the "strathclyde methodology" in aqueous emulsion. Macromolecules 39, 1455–1460.
Blanazs, A., Armes, S.P., Ryan, A.J., 2009. Self-assembled block copolymer aggregates: From micelles to vesicles and their biological applications. Macromol. Rapid Commun. 30, 267–277.
Constantinou, A.P., Georgiou, T.K., 2016. Tuning the gelation of thermoresponsive gels. Eur. Polym. J. 78, 366–375.
Cook, M.T., Haddow, P., Kirton, S.B., McAuley, W.J., 2021. Polymers Exhibiting Lower Critical Solution Temperatures as a Route to Thermoreversible Gelators for Healthcare. Adv. Funct. Mater. 31, 2008123.
Da Silva, M.A., Bode, F., Grillo, I., Dreiss, C.A., 2015. Exploring the Kinetics of Gelation and Final Architecture of Enzymatically Cross-Linked Chitosan/Gelatin Gels. Biomacromolecules. 16, 1401–1409.
da Silva, M.A., Haddow, P., Kirton, S.B., McAuley, W.J., Porcar, L., Dreiss, C.A., Cook, M. T., 2022. Thermoresponsive Triblock-Copolymers of Polyethylene Oxide and Polymethacrylates: Linking Chemistry, Nanoscale Morphology, and Rheological Properties. Adv. Funct. Mater. 32, 2109010.
Da Silva, M.A., Rajbanshi, A., Opoku-achampong, D., Mahmoudi, N., Porcar, L., Gutfreund, P., Tummino, A., Maestro, A., Dreiss, C.A., Cook, M.T., 2022. Engineering Thermoresponsive Emulsions with Branched Copolymer Surfactants. Macromol. Mater. Eng. 307, 2200321.

Dickinson, E., Casanova, H., 1999. A thermoreversible emulsion gel based on sodium caseinate. Food Hydrocoll. 13, 285–289.
Dumortier, G., Grossiord, J.L., Agnely, F., Chaumeil, J.C., 2006. A review of poloxamer 407 pharmaceutical and pharmacological characteristics. Pharm. Res. 23, 2709–2728.
FDA, n.d. Inactive Ingredient Database for Approved Drug Products [WWW Document]. URL www.accessdata.fda.gov (accessed 1.4.23).
Feigin, L.A., Svergun, D.I., 1987. Structure Analysis by Small-Angle X-Ray and Neutron Scattering, 1st ed. Springer, New York LLC.
Haddow, P.J., da Silva, M.A., Kaldybekov, D.B., Dreiss, C.A., Hoffman, E., Hutter, V., Khutoryanskiy, V.V., Kirton, S.B., Mahmoudi, N., McAuley, W.J., Cook, M.T., 2021. Polymer Architecture Effects on Poly(N, N-Diethyl Acrylamide)-b-Poly(Ethylene Glycol)-b-Poly(N, N-Diethyl Acrylamide) Thermoreversible Gels and Their Evaluation as a Healthcare Material. Macromol. Biosci. 22, 2100432.
Haddow, P., McAuley, W.J., Kirton, S.B., Cook, M.T., 2020. Poly(N-isopropyl acrylamide)-b-poly(ethylene glycol)-b-poly(N-isopropyl acrylamide) as a thermoreversible gelator for topical administration. Mater. Adv. 1, 371–386.
Hammouda, B., Ho, D.L., Kline, S., 2004. Insight into clustering in poly(ethylene oxide) solutions. Macromolecules 37, 6932–6937.
Heenan, R.K., Penfold, J., King, S.M., 1997. SANS at Pulsed Neutron Sources: Present and Future Prospects. J. Appl. Crystallogr. 30, 1140–1147.
Hu, Y., Ting, Y., Hu, J., Hsieh, S., 2016. Techniques and methods to study functional characteristics of emulsion systems. J. Food Drug Anal. 25, 16–26.
Hussain, A., Ahsan, F., 2005. The vagina as a route for systemic drug delivery. J. Control. 103, 301–313.
Jeong, B., Kim, S.W., Bae, Y.H., 2012. Thermosensitive sol-gel reversible hydrogels. Adv. Drug Deliv. Rev. 64, 154–162.
Koh, A.Y.C., Saunders, B.R.R., 2000. Thermally induced gelation of an oil-in-water emulsion stabilised by a graft copolymer. Chem. Commun. 6, 2461–2462.
Kolouchova, K., Groborz, O., Slouf, M., Herynek, V., Parmentier, L., Babuka, D., Cernochova, Z., Koucky, F., Sedlacek, O., Hruby, M., Hoogenboom, R., Vlierberghe, S.V., 2022. Thermoresponsive Triblock Copolymers as Widely Applicable Magnetic Resonance Imaging Tracers. Chem. Mater. 34, 10902–10916.
Kotlarchyk, M., Chen, S.H., 1983. Analysis of small angle neutron scattering spectra from polydisperse interacting colloids. J. Chem. Phys. 79, 2461–2469.
Li, Z., Geisel, K., Richtering, W., Ngai, T., 2013. Poly(N-isopropylacrylamide) microgels at the oil–water interface: adsorption kinetics. Soft Matter 9, 9939–9946.
McClements, D.J., Jafari, S.M., 2018. Improving emulsion formation, stability and performance using mixed emulsifiers: A review. Adv. Colloid Interface Sci. 251, 55–79.
Meewes, M., Ricka, J., de Silva, M., Nyffenegger, R., Binkert, T., 1991. Coil-Globule Transition of Poly(N-isopropylacrylamide). A Study of Surfactant Effects by Light Scattering. Macromolecules 24, 5811–5816.
Rajbanshi, A., da Silva, M.A., Murnane, D., Porcar, L., Dreiss, C.A., Cook, M.T., 2022. Polymer architecture dictates thermoreversible gelation in engineered emulsions stabilised with branched copolymer surfactants. Polym. Chem. 13, 5730–5744.
Scherlund, M., Malmsten, M., Brodin, A., 1998. Stabilization of a thermosetting emulsion system using ionic and nonionic surfactants. Int. J. Pharm. 173, 103–116.
Schulman, J.H., Cockbain, E.G., 1940. Molecular Interactions at Oil / Water Interfaces. Trans. Faraday Soc. 35, 651–661.
Shiao, S.Y., Chhabra, V., Patist, A., Free, M.L., Huibers, P.D.T., Gregory, A., Patel, S., Shah, D.O., 1998. Chain length compatibility effects in mixed surfactant systems for technological applications. Adv. Colloid Interface Sci. 74, 1–29.
Skvarla, J., Zednik, J., Slouf, M., Pispas, S., Stepanek, M., 2014. Poly(N-isopropyl acrylamide)-block-poly(n-butyl acrylate) thermoresponsive amphiphilic copolymers: Synthesis, characterization and self-assembly behavior in aqueous solutions. Eur. Polym. J. 61, 124–132.
Stepanek, M., Hajduova, J., Prochazka, K., Slouf, M., Nebesarova, J., Mountrichas, G., Mantzaridis, C., Pispas, S., 2012. Association of Poly (4-hydroxystyrene) - block -Poly (Ethylene oxide) in Aqueous Solutions : Block Copolymer Nanoparticles with Intermixed Blocks. Langmuir 28, 307–313.
Swindle-Reilly, K.E., Shah, M., Hamilton, P.D., Eskin, T.A., Kaushal, S., Ravi, N., 2009. Rabbit study of an in situ forming hydrogel vitreous substitute. Investig. Ophthalmol. Vis. Sci. 50, 4840–4846.
SasView version 4.2.2 [https://www.sasview.org/], n.d.
NIST SLD Calculator [WWW Document], URL https://www.ncnr.nist.gov/resources/sldcalc.html (accessed 4.20.21).
USP Monographs: Emulsifying Wax [WWW Document], 2008. . United States Pharmacopeoia. URL http://www.pharmacopeia.cn/v29240/usp29nf24s0_m88980.html.
Ward, M.A., Georgiou, T.K., 2011. Thermoresponsive polymers for biomedical applications. Polymers (Basel) 3, 1215–1242.
Weaver, J.V.M., Rannard, S.P., Cooper, A.I., 2009. Polymer-Mediated Hierarchical and Reversible Emulsion Droplet Assembly. Angew. Chemie 121, 2165–2168.
Wignall, G.D., Bates, F.S., 1987. Absolute calibration of small-angle neutron scattering data. J. Appl. Crystallogr. 20, 28–40.
Woodward, R.T., Slater, R.A., Higgins, S., Rannard, S.P., Cooper, A.I., Royles, B.J.L., Findlay, P.H., Weaver, J.V.M., 2009. Controlling responsive emulsion properties via polymer design. Chem. Commun. 3554–3556.
Yara-Varón, E., Li, Y., Balcells, M., Canela-Garayoa, R., Fabiano-Tixier, A.S., Chemat, F., 2017. Vegetable oils as alternative solvents for green oleo-extraction, purification and formulation of food and natural products. Molecules 22, 1–24.
Zhang, J., Pelton, R., 1996. Poly(N-isopropylacrylamide) at the Air/Water Interface. Langmuir 12, 2611–2612.
Zhao, Y., Cao, Y., Yang, Y., Wu, C., 2003. Rheological study of the sol-gel transition of hybrid gels. Macromolecules 36, 855–859.
Zhao, Y.Z., Jiang, X., Xiao, J., Lin, Q., Yu, W.Z., Tian, F.R., Mao, K.L., Yang, W., Wong, H. L., Lu, C.T., 2016. Using NGF heparin-poloxamer thermosensitive hydrogels to enhance the nerve regeneration for spinal cord injury. Acta Biomater. 29, 71–80.